LETTER • OPEN ACCESS

Hydrothermal carbon release to the ocean and atmosphere from the eastern equatorial Pacific during the last glacial termination

View the article online for updates and enhancements.

Environmental Research Letters

LETTER

Hydrothermal carbon release to the ocean and atmosphere from the eastern equatorial Pacific during the last glacial termination

Lowell D Stott[1] , Kathleen M Harazin[2] and Nadine B Quintana Krupinski[3]

[1] Department of Earth Sciences, University of Southern California, United States of America
[2] Research School of Earth Sciences, The Australian National University, Australia
[3] Department of Geology, Lund University, Sweden

E-mail: stott@usc.edu

Abstract

Arguably among the most globally impactful climate changes in Earth's past million years are the glacial terminations that punctuated the Pleistocene epoch. With the acquisition and analysis of marine and continental records, including ice cores, it is now clear that the Earth's climate was responding profoundly to changes in greenhouse gases that accompanied those glacial terminations. But the ultimate forcing responsible for the greenhouse gas variability remains elusive. The oceans must play a central role in any hypothesis that attempt to explain the systematic variations in pCO_2 because the Ocean is a giant carbon capacitor, regulating carbon entering and leaving the atmosphere. For a long time, geological processes that regulate fluxes of carbon to and from the oceans were thought to operate too slowly to account for any of the systematic variations in atmospheric pCO_2 that accompanied glacial cycles during the Pleistocene. Here we investigate the role that Earth's hydrothermal systems had in affecting the flux of carbon to the ocean and ultimately, the atmosphere during the last glacial termination. We document late glacial and deglacial intervals of anomalously old ^{14}C reservoir ages, large benthic-planktic foraminifera ^{14}C age differences, and increased deposition of hydrothermal metals in marine sediments from the eastern equatorial Pacific (EEP) that indicate a significant release of hydrothermal fluids entered the ocean at the last glacial termination. The large ^{14}C anomaly was accompanied by a ~4-fold increase in Zn/Ca in both benthic and planktic foraminifera that reflects an increase in dissolved [Zn] throughout the water column. Foraminiferal B/Ca and Li/Ca results from these sites document deglacial declines in $[CO_3{}^{2-}]$ throughout the water column; these were accompanied by carbonate dissolution at water depths that today lie well above the calcite lysocline. Taken together, these results are strong evidence for an increased flux of hydrothermally-derived carbon through the EEP upwelling system at the last glacial termination that would have exchanged with the atmosphere and affected both $\Delta^{14}C$ and pCO_2. These data do not quantify the amount of carbon released to the atmosphere through the EEP upwelling system but indicate that geologic forcing must be incorporated into models that attempt to simulate the cyclic nature of glacial/interglacial climate variability. Importantly, these results underscore the need to put better constraints on the flux of carbon from geologic reservoirs that affect the global carbon budget.

1. Introduction-recent discoveries and motivation for this study

There have been several hypotheses put forth over the years to account for the systematic variations in atmospheric pCO_2 that accompanied glacial/interglacial cycles during the Pleistocene (Berger 1982, Archer *et al* 2000, Sigman and Boyle 2000, Lund and Asimow 2011, Stott and Timmermann 2011, Broecker *et al* 2015, Huybers and Langmuir 2017). Yet, after more than four decades of scientific effort to evaluate these hypotheses and identify the ultimate cause or causes of the
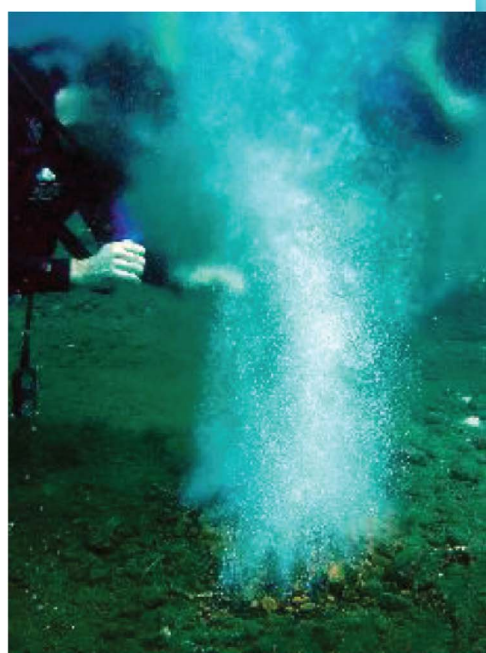
Figure 1. Nearly pure CO_2 bubbles emanating from sediments that blanket an active hydrothermal system in the western tropical Pacific. Photos by Roy Price, courtesy of Jan Amend.

greenhouse gas variations, the answer remains elusive. This likely reflects the fact that no single mechanism acting alone appears capable of explaining all aspects of carbon cycle behavior that accompanied the glacial cycles (Fischer *et al* 2010). For example, recent discoveries indicate marine carbon budgets underestimate the amount of carbon entering the oceans from hydrothermal systems. This is because over the past two decades reservoirs of liquid and hydrate CO_2 have been discovered in rocks and sediments that blanket the margins of some active marine hydrothermal vents (Sakai *et al* 1990, Inagaki *et al* 2006, Lupton *et al* 2006, Lupton *et al* 2008). In the back arc basin of the Okinawa Trough a 'lake' of liquid CO_2 accumulates beneath a cap of CO_2-hydrate (Inagaki *et al* 2006, Nealson 2006) and at shallower ocean depths pure CO_2 gas is observed to emanate directly from sediments that blanket the margins of hydrothermal vents (figure 1). Pools of liquid CO_2 have been discovered in the Aegean Sea (Camilli *et al* 2015). Geologic carbon reservoirs such as these are not explicitly included in current marine carbon budgets. In fact, quantifying how carbon from sediment and rock-hosted reservoirs contributes to the overall marine carbon budget is not yet possible because there are too few observations and virtually no *in situ* measurements of the CO_2 flux from these types of reservoirs (Burton *et al* 2013). Yet, in one remarkable study, Lupton *et al* (2008) were able to quantify the flux of liquid CO_2 from a sediment/rock-hosted reservoir at a site on Mariana trench in the western Pacific by observing the rate that bubbles of pure liquid CO_2 emanate from a small opening on the seafloor. They

estimated the carbon flux from this single opening to be 0.1% of the entire Mid Ocean Ridge flux. When Lupton *et al* (2008) documented the gas and liquid phases in the western Pacific, they pointed out that of the hundreds of vents thus far investigated, only a few were found to have a separate CO_2 phase, concluding this must be a rare circumstance and perhaps limited to volcanic arcs. However, investigations targeting CO_2 fluxes from the cool flanks of active hydrothermal sites has not been a priority and observations are therefore sparse (Burton *et al* 2013). With only about one-third of the global ocean spreading ridges surveyed, vast portions of the sea floor have not been investigated at all (Beaulieu *et al* 2015). Even if only a small percentage of the unsampled hydrothermal systems contain separate gas or liquid CO_2 phases it could change the global marine carbon budget substantially (Burton *et al* 2013). Importantly, where these reservoirs have been found at shallow-intermediate depths, the flux from the sediment and rock reservoirs is modulated by a density-stratified boundary layer at the sediment/water interface where a thin layer of CO_2 saturated-seawater and CO_2 hydrate forms (Inagaki *et al* 2006, Lupton *et al* 2006). The boundary layer is sensitive to temperature changes. Reservoirs of carbon like this can exist at deep water depths but may be less sensitive to temperature changes.

Stott and Timmermann (2011) were motivated by the observations described above to consider whether the large deglacial radiocarbon $\Delta^{14}C$ excursions documented from biogenic carbonates in the eastern Pacific and Indian Oceans (Marchitto *et al* 2007, Stott *et al*

2009, Bryan *et al* 2010) could be indicative of past episodes of geologic carbon release from hydrothermal sources. The magnitude of the deglacial $\Delta^{14}C$ excursions in the eastern equatorial Pacific (EEP) core VM21-30 are too large to be explained by ventilation of a previously isolated deep-water mass. Furthermore, similarly large $\Delta^{14}C$ anomalies are not found at other intermediate depth sites bathed by the same water mass (De Pol-Holz *et al* 2010, Ronge *et al* 2016). Given this, Stott and Timmermann (2011) reasoned that the magnitude and duration of the excursion in the EEP would have required a sustained input of ^{14}C-dead carbon from a localized source, the most likely being a hydrothermal source in the EEP. There are several volcanic provinces located within the EEP that could have potentially contributed carbon-rich hydrothermal fluids, including the Galapagos Hot Spot (Christopher *et al* 2013, Harpp and White 2018), the Galapagos Spreading Center, the Cocos Ridge, the Carnegie Ridge and perhaps the submerged margins of the Central American Arc. If a substantial release of geologic carbon to the upper ocean occurred in the EEP from one or more of these volcanic sources, it has important implications for reconciling why there was a large decrease in atmospheric $\Delta^{14}C$ during the glacial termination when other cosmogenic radionuclides did not (Muscheler *et al* 2004, Petrenko *et al* 2016) because the EEP is a primary conduit for exchange of carbon from the ocean to the atmosphere (Takahashi *et al* 2009).

The original Stott and Timmermann (2011) hypothesis met with considerable skepticism because few paleoceanographers were aware of the recent discoveries of geologic reservoirs of CO_2 in the ocean or that hydrothermalism may have varied on glacial/interglacial timescales. But over the past several years other studies have begun to consider ways that geologic carbon could have influenced glacial/interglacial CO_2 and climate variability (Lund and Asimow 2011, Broecker *et al* 2015, Tolstoy 2015, Lund *et al* 2016, Ronge *et al* 2016, Huybers and Langmuir 2017). The seafloor discoveries and the hypotheses summarized above pose challenges to the paleoceanography community to effectively evaluate whether geologic processes contributed significantly to the systematic variations in atmospheric pCO_2 that accompanied each glacial/interglacial cycle over the past million years. In the present study we evaluated further the suggestion by Stott and Timmermann that the large $\Delta^{14}C$ anomalies in the EEP were due to a release of hydrothermal carbon during the last glacial termination. We emphasize that the current study does not attempt to identify the specific site of hydrothermal carbon release. There are multiple sites in the EEP where hydrothermal and volcanic activity is known. And while there have been various studies of active hydrothermalism in the EEP, there is a significant amount of area in the EEP that has not been explored. The Galapagos island chain itself is an active volcanic

center as is the EPR. The flanks of the Central American Arc are also known to emit large amounts of CO_2 through the sediments that blanket the margins of the arc (Salazar *et al* 2001). Hence, there are large gaps in knowledge about where CO_2 is emitted in the EEP. We also emphasize that this study is not an attempt to identify a specific phase of CO_2 released to the ocean at the glacial termination. That topic is beyond the scope of this effort. The primary intent here is to further evaluate the suggestion by Stott and Timmermann (2011) that hydrothermal carbon was released to the ocean in the EEP during at the last glacial termination and hydrothermal carbon contributed to the very large $\Delta^{14}C$ anomalies observed in marine sediments. The Stott and Timmermann hypothesis made several predictions about carbonate chemistry and carbonate preservation in the EEP during the last glacial termination. An evaluation of those predictions here is one step in an effort to evaluate if and how geologic sources of carbon contributed significantly to the glacial/interglacial carbon cycle variability.

2. Methods

A complete description of the analytical methods used in this study is provided in the supplementary section. The Stott and Timmermann hypothesis predicts that if there was a release of hydrothermal carbon of sufficient quantity to produce the large ^{14}C age anomalies in the EEP it would have changed the carbonate chemistry and affected calcite and aragonite preservation. It may have also left a trace metal fingerprint of hydrothermal elements on the sediments. We demonstrate that large benthic-planktic ^{14}C age differences originally documented in the VM21-30 core by Stott *et al* (2009) are observed in other cores from the EEP (figure 2; table 1). We also demonstrate that the surface ocean reservoir age varied significantly across the EEP during the glacial termination with the largest increase in surface ocean reservoir age of more than 6000 years, just south of the equator within the zone of upwelling.

Variability in the ocean carbonate system and carbonate preservation has been evaluated using scanning electron microscopy to inspect carbonates for signs of dissolution. The weight and abundance of *Orbulina universa*, a planktic foraminifera, is quantified because changes in the shell weight of individual *O. universa* has been shown to correlate positively with carbonate ion concentration $[CO_3^{2-}]$ (Bijma *et al* 1999, Bijma *et al* 2002). B/Ca, Li/Ca, and Zn/Ca of planktic and benthic foraminifera were measured to assess changes in ambient seawater carbonate chemistry. B/Ca has been investigated as a proxy for carbonate system parameters in planktic foraminifera (Yu *et al* 2007, Foster 2008, Hendry *et al* 2009, Allen *et al* 2012, Yu *et al* 2013, Holland *et al* 2017, Howes *et al* 2017, Quintana Krupinski *et al* 2017). B/Ca is particularly useful because in some species it is unaffected by
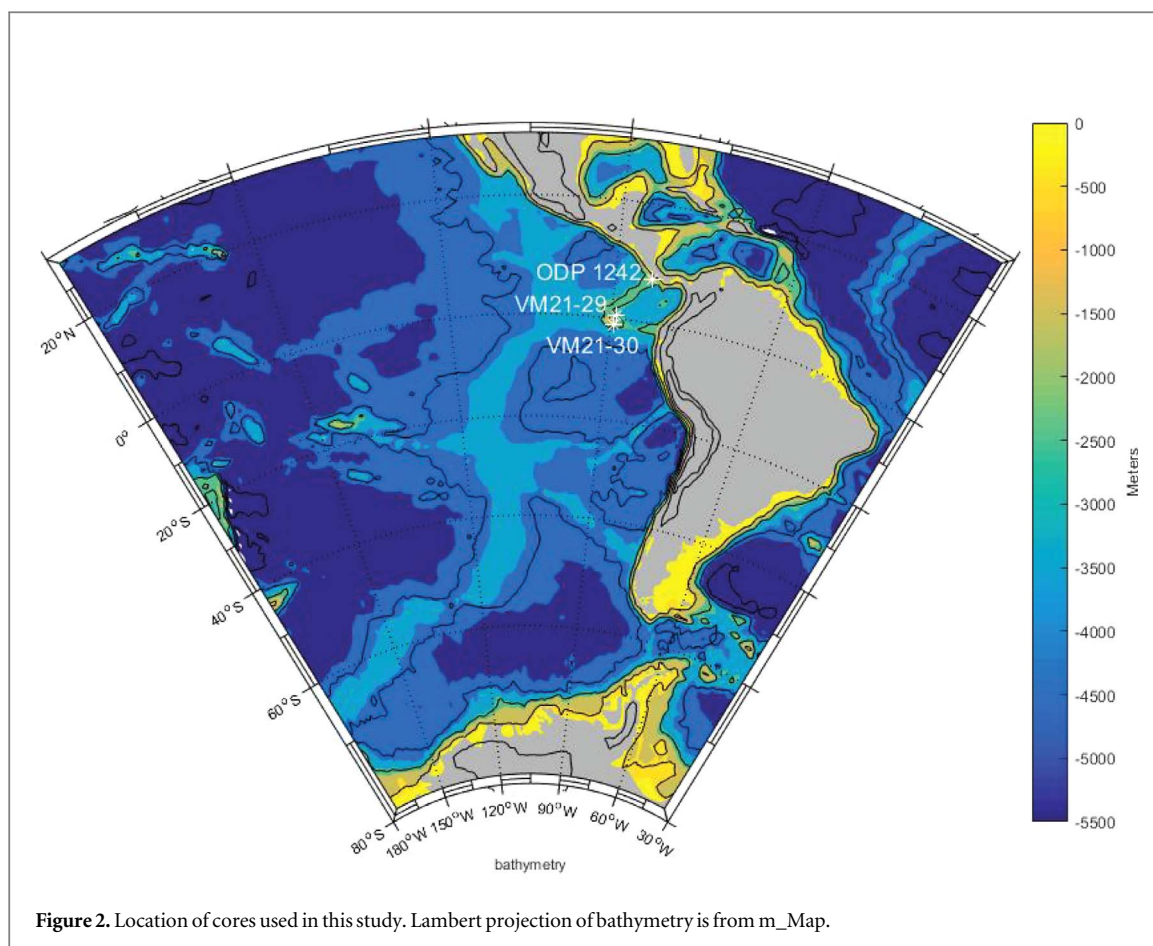
Figure 2. Location of cores used in this study. Lambert projection of bathymetry is from m_Map.

Table 1. Sediment cores used in the study.

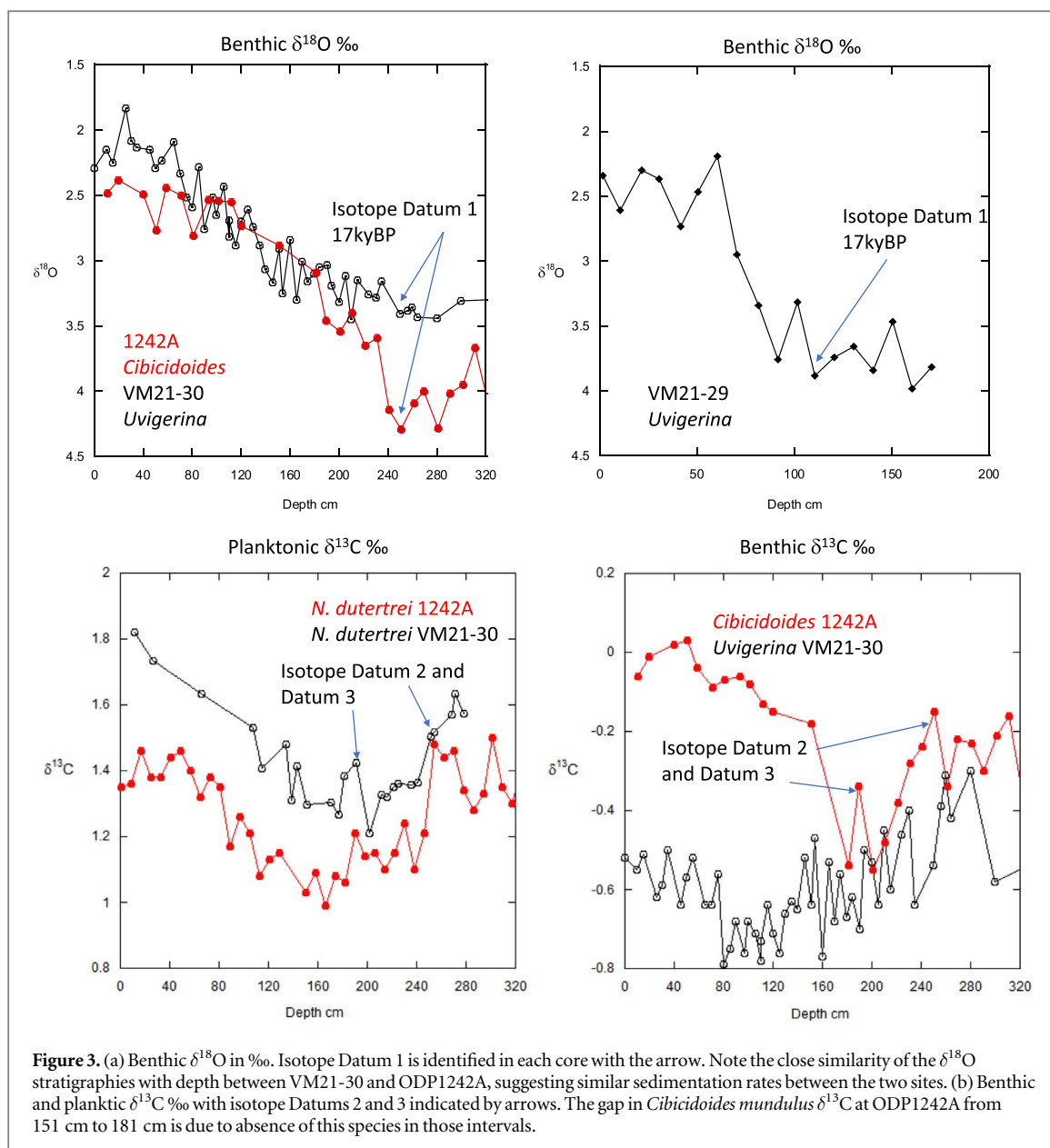| Core location	Latitude	Longitude	Water depth (m)
VM21-30	−1.22	−89.68	617
VM21-29	0.95	−89.35	712
ODP 1242A	7.86	−106.61	1364

dissolution or temperature (Wara *et al* 2003, Foster 2008, Henehan *et al* 2015, Dai *et al* 2016, Haynes *et al* 2017, Quintana Krupinski *et al* 2017), including *Neogloboquadrina dutertrei* and *Neogloboquadrina incompta* that are studied here.

Li/Ca has been less utilized as a proxy for $[CO_3^{2-}]$ because of the opposing effects of $[CO_3^2]$ and temperature on Li incorporation into the foraminiferal calcite. Similar to B/Ca, Li/Ca has been shown to have a positive correlation with carbonate saturation state ($\Delta[CO_3^{2-}]$, defined as $\Delta[CO_3^{2-}] = [CO_3^{2-}]_{in\ situ} - [CO_3^{2-}]_{saturation}$) although unlike B/Ca (which is not influenced by temperature), Li/Ca exhibits an inverse relationship with temperature (Hall and Chan 2004, Marriott *et al* 2004, Lear and Rosenthal 2006, Bryan and Marchitto 2008, Lear *et al* 2010, Doss *et al* 2018). Therefore, concomitant changes in temperature and $\Delta[CO_3^{2-}]$ can be obfuscated in Li/Ca, even though the Li/Ca-temperature relationship is weaker in planktic foraminifera (Hall and Chan 2004, Hathorne and James 2006). When paired

with temperature proxies (Mg/Ca, alkenones) and other carbonate system proxies (e.g. B/Ca), Li/Ca can be used to deconvolve various influences.

Core top studies have suggested that Zn/Ca in benthic foraminiferal calcite also covaries with $[CO_3^{2-}]$ (Marchitto *et al* 2000, 2002, van Dijk *et al* 2017). However, unlike Li and B, Zn behaves non-conservatively in the ocean and has a refractory nutrient-type distribution with a relatively shorter oceanic residence time (<50 kyr). Additionally, Zn incorporation is proportional to seawater [Zn] (Boyle 1981, Marchitto *et al* 2000, Marchitto *et al* 2002), and therefore, Zn/Ca is sensitive to both $[CO_3^2]$ and changes in seawater [Zn]. This is important in the present study because $[Zn]_{sw}$ is a tracer of hydrothermal flux (Levin *et al* 2016). However, in low calcite-saturation conditions (e.g. some benthic foraminiferal environments), under-saturation ($\Delta[CO_3^{2-}]$) can also affect Zn/Ca. Therefore, to use Zn/Ca to reconstruct past ocean $[Zn]_{sw}$ requires an independent estimate of seawater $[CO_3^2]$ (Marchitto *et al* 2002, van Dijk *et al* 2017). For this reason, we combine measurements of Zn/Ca with both B/Ca and Li/Ca to deconvolve the influences of seawater [Zn] from changes in $[CO_3^{2-}]$.

We quantified changes in accumulation of hydrothermal elements in oxide overgrowths precipitated on the carbonate sediments in the EEP by analyzing uncleaned foraminifera from the late glacial and deglacial sections of two cores. This is not an effort to

Figure 3. (a) Benthic δ^{18}O in ‰. Isotope Datum 1 is identified in each core with the arrow. Note the close similarity of the δ^{18}O stratigraphies with depth between VM21-30 and ODP1242A, suggesting similar sedimentation rates between the two sites. (b) Benthic and planktic δ^{13}C ‰ with isotope Datums 2 and 3 indicated by arrows. The gap in *Cibicidoides mundulus* δ^{13}C at ODP1242A from 151 cm to 181 cm is due to absence of this species in those intervals.

quantify actual fluxes of hydrothermal metals but rather to assess whether there was increased accumulation of hydrothermal metals across the glacial termination.

3. Results

3.1. Variable ^{14}C reservoir ages

Previous studies suggest that there were large changes in ocean reservoir ages in the EEP during the last glacial termination (Stott *et al* 2009, de la Fuente *et al* 2015, Umling and Thunell 2017). The reason for the reservoir age variability is of interest here. The benthic stable isotope stratigraphies document several 'isotope-events' that are seen in both Antarctic ice core records and in composite reconstructions of benthic δ^{18}O (Stern and Lisiecki 2014). These events are used to estimate how reservoir ages varied by comparing these isotope chronologic events with their

corresponding ^{14}C age. The events include the initial δ^{18}O decrease that marked the onset of the last deglaciation (figure 3(A)) and a negative δ^{13}C excursion centered on the deglaciation (figure 3(B)). This δ^{13}C excursion was documented previously in planktic foraminifera (Spero and Lea 2002, Bostock *et al* 2004) and in atmospheric CO_2 extracted from Antarctic ice cores where it has a well-established chronology (Schmitt *et al* 2012) (figure S1 is available online at stacks.iop.org/ERL/14/025007/mmedia). In the ice core record the deglacial δ^{13}C excursion began at 17.2 kyBP $\pm\sim$500 years and the first δ^{13}C minima was at 15.8 kyBP $\pm\sim$500 years (Schmitt *et al* 2012). The magnitude of this initial δ^{13}C decrease in the EEP foraminiferal δ^{13}C records is $\sim$−0.4‰, as it is in the ice core record. There was a second δ^{13}C minimum at 12.3ky BP in the ice core record but this minima is not distinguishable in our cores, even though it is well-resolved in the higher resolution records from the

Table 2. Stable isotope intervals used as chronologic datums.

Sediment core	Datum 1 (17.0 ky BP)	Datum 2 (17.2 ky BP)	Datum 3 (13.5 ky BP)
VM21-30	235 cm	251 cm	190 cm
VM21-29	110 cm	120 cm?	~60 cm
ODP 1242A	241 cm	251 cm	189 cm

western equatorial Pacific (Stott *et al* 2004, 2009). Here we use the mid-point of the $\delta^{13}C$ excursion as a chronologic datum, which has a mean calendar age of 13.5 ky BP (figure S1).

The $\delta^{13}C$ excursions (Datums 2 and 3) are also observed in the EEP benthic stratigraphies (figure 3(B)). The early-deglacial $\delta^{13}C$ excursion in the *Cibicidoides* record from ODP1242A stands out distinctly against the long-term $\delta^{13}C$ increase that characterizes the later deglacial section (figure 3(B)). In the *Uvigerina* record from VM21-30 there is longer-term decrease in $\delta^{13}C$ that extends through the entire deglacial interval. We know of no other intermediate depth cores in the Pacific that record a comparable *Cibicidoides* $\delta^{13}C$ excursion. It appears this benthic $\delta^{13}C$ excursion is a local signal.

The depth and age of each of the isotope datums are listed in table 2. Large reservoir age corrections are required to bring ^{14}C-based calendar ages (particularly in VM21-30) into agreement with the stable isotope datums. For example, the onset in benthic $\delta^{18}O$ decrease marking the beginning of deglaciation (Datum 1) occurs at the same depth in both ODP1242A and VM21-30 (figure 3(A)). The beginning of the deglacial $\delta^{13}C$ excursion (Datum 2) also occurs at the same depth in both cores (figure 3(B)). In fact, the late glacial and deglacial stable isotope stratigraphies of both cores are very similar and this implies they share a similar sediment accumulation rate.

This is important because the deglacial ^{14}C stratigraphies of these two cores are very different. In figure 4 the calendar age for each of the three datums is plotted versus its depth in ODP 1242A and VM21-30. The planktic radiocarbon ages shown in figure 5 were converted to calendar age using Calib 7.1 (Reimer *et al* 2013) with ΔR of 425 ± 200 years. Increasing ΔR from 0 to 425 years brings the ^{14}C calendar ages in the ODP1242A record into agreement with the datum ages. This implies that reservoir ages in the EEP near ODP 1242A were at least 400 years older during the deglaciation than during the late Holocene (Benway *et al* 2006). However, even more dramatic changes in reservoir age are evident in the VM21-30 record (figure 4) where the offset between the stable isotope datums and the ^{14}C calendar ages is as much as 6000 years. For example, the initial benthic $\delta^{18}O$ decrease (Datum 1) in VM21-30 occurs at 250 cm. The ^{14}C-based calendar age for this horizon (with $\Delta R = 425$ years) is 22 kyBP, nearly 5000 years older than the age of this same $\delta^{18}O$ horizon in the

ODP1242A core and in other benthic foraminiferal records from the Pacific (Stern and Lisiecki 2014). The oldest surface reservoir ages at the VM21-30 site was during the latest glacial and early deglacial. The accumulation rate of VM21-29 is much lower than the other two core and hence, it is more difficult to place the exact horizon of the isotope datums in this core.

3.2. Benthic-planktic ^{14}C age differences

Stott *et al* (2009) documented large benthic-planktic ^{14}C age differences (B-P ages) in the glacial and deglacial section of VM21-30. The B-P ages are >4000 years in most intervals of the core between 100 and 300 cm, spanning late glacial and deglacial sections (figure 5). Anomalously large B-P ^{14}C ages are also observed in ODP 1242A and VM21-29 (figure 5). The B-P ^{14}C ages are highest in the late glacial section of ODP 1242A core and began to increase at about the same time as at the VM21-30 site. However, at the ODP 1242A site, the large B-P ages did not persist through the deglaciation.

In VM21-29 the B-P ^{14}C ages are also anomalously large between ~200 and 75 cm, which corresponds to the late glacial and deglacial section (figure 5). The B-P ^{14}C ages from these intervals are between 2000 and 5000 years whereas the Holocene B-P ^{14}C age differences are similar to modern. Putting the data from all three cores together suggests that there were large increases in benthic-planktic age difference across the EEP during the latest glacial and deglacial, but the largest changes occurred at the equator, near VM21-30 and VM21-29, during the deglaciation.

3.3. Carbonate preservation

A visual inspection of the core samples documents variable changes in the preservation and abundance of benthic and planktic foraminifera in the late glacial and deglacial sections of all three cores (table S7). Aragonitic pteropods are present throughout late glacial and Holocene, although their abundance and preservation varies between samples. At 254.8 cm in VM21-30 for example, the abundance of aragonite is very low but pteropods are intact and whole. Yet, in this same sample some of the calcitic benthic and planktic foraminifera are partially dissolved (figure 6). At the 268.5 cm horizon pteropods are very abundant and benthic shells are well-preserved but the B-P ^{14}C ages are approximately 4000 years.

The VM21-29 core also exhibits variable carbonate preservation and abundances in the late glacial and deglacial sections (table S7). The aragonite and carbonate are abundant and well-preserved between 170 and 150 cm, which corresponds to the latest glacial. Directly above this interval, at the onset of the deglacial, aragonite abundance drops significantly and some of the benthic foraminifera are partially dissolved. Above 100 cm (midway through the deglacial section) carbonate preservation is good and aragonite
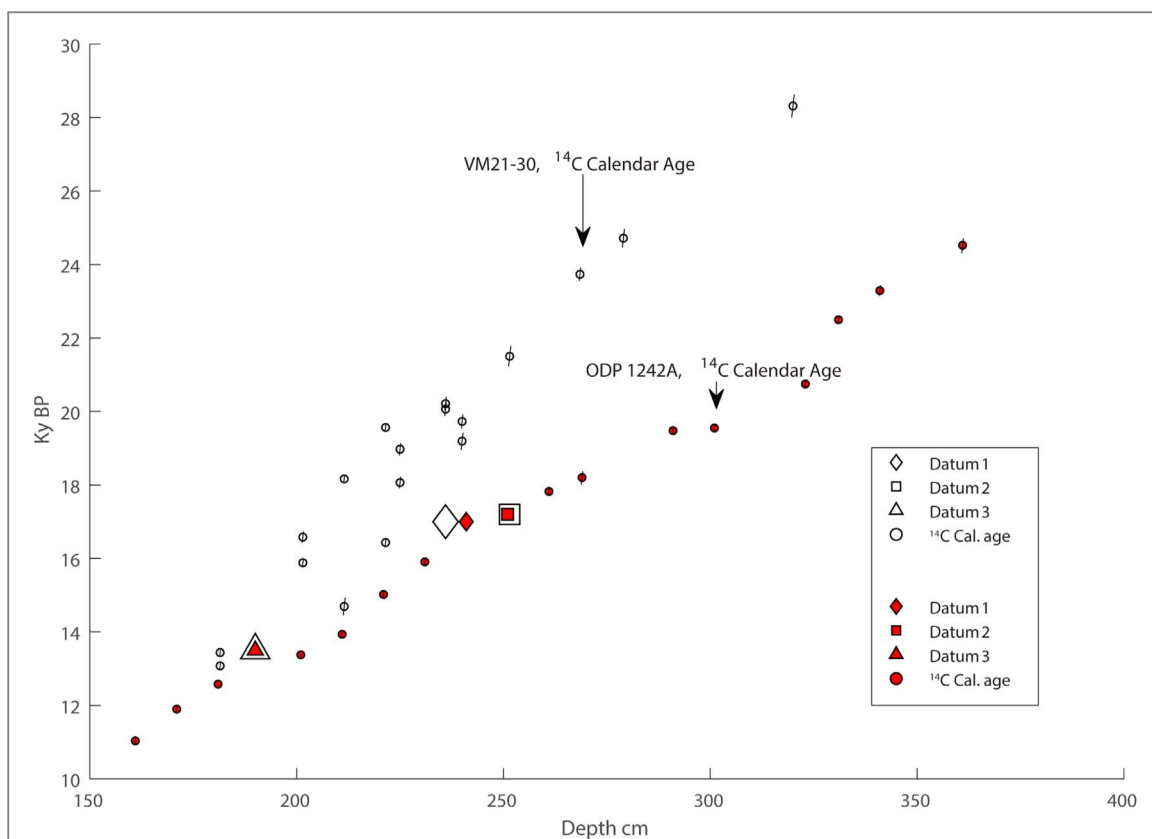
Figure 4. Comparison of ^{14}C calendar ages ($\Delta R = 422$ year) in ODP1242A (red) and VM21-30 (open symbols) with isotope datums (as shown in figures 3(A), (B)) indicated as diamonds, squares or triangles. Calendar age uncertainties ($\pm$) are shown as vertical bars. A nominal depth uncertainty of 10 cm is applied to the datums because this is the approximate separation between adjacent samples. Note the large offset in ^{14}C calendar ages relative to isotope datums in VM21-30.
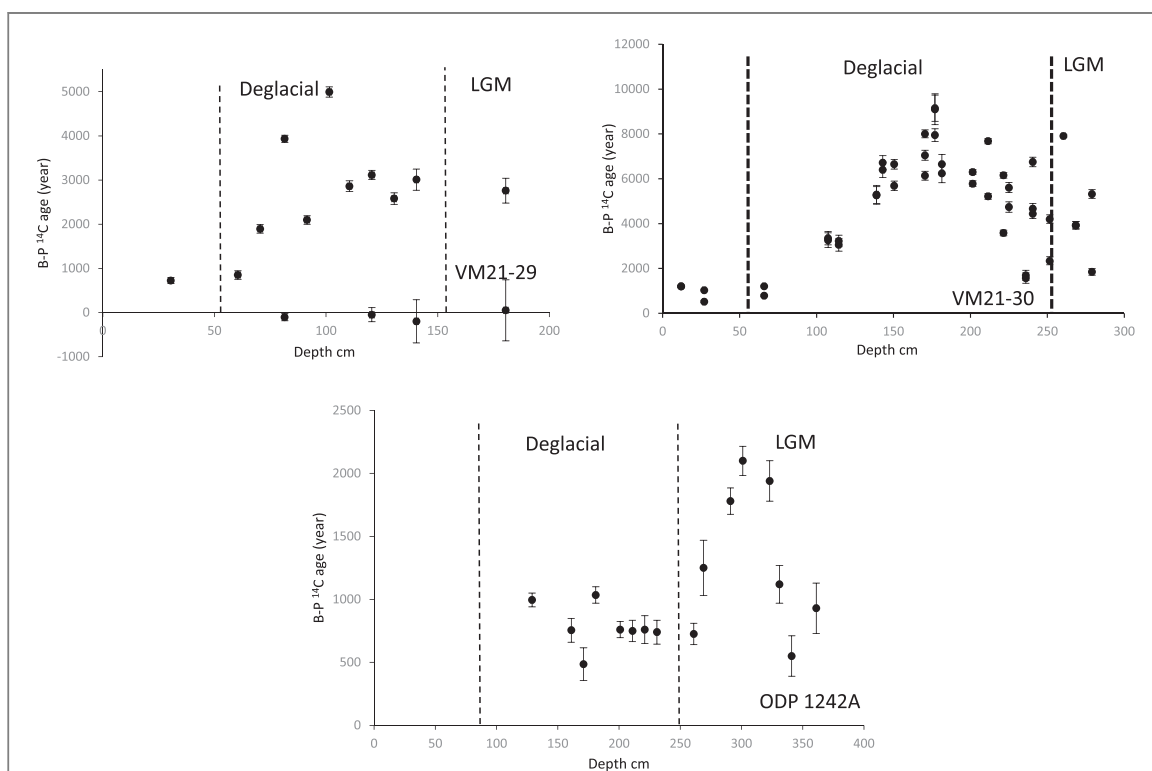
Figure 5. Benthic-planktonic raw ^{14}C age differences for cores VM21-29, VM21-30 and ODP1242A. Error bars are the sum of the raw ^{14}C age uncertainties for the benthic and planktic foram. Vertical dashed lines mark the boundaries between Last Glacial Maximum (LGM), the last deglacial, and the Holocene.
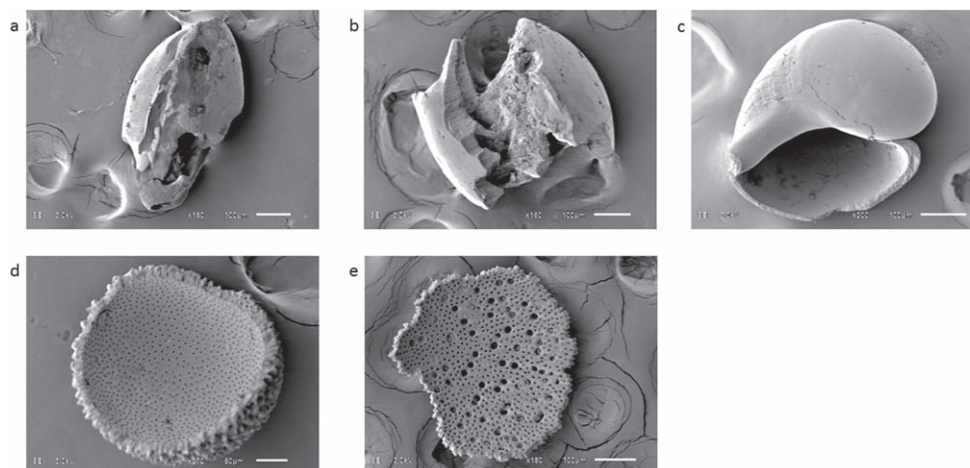
Figure 6. SEM photomicrographs of partially-dissolved benthic foraminifera (a), (b) and intact pteropod (c) from VM21-30, 254.8 cm. Well-preserved glacial final chamber ODP 1242A, 330 cm (d) and partially dissolved deglacial final chamber ODP 1242A, 210 cm (e).

is abundant. From these observations, it appears that only the early deglacial section of VM21-29 exhibits lower carbonate preservation whereas in the VM21-30 core the variable carbonate preservation and abundances persists from the late glacial through the entire deglacial section.

Visual comparison of ODP1242A samples with those from VM21-30 and VM21-29 is difficult because the ODP samples contain a much higher clay content and the samples are indurated. However, several important observations stand out. In this core the calcite foraminifera are abundant, intact and well-preserved below 441 cm, which corresponds to the late glacial. Foraminiferal abundances drop, and preservation declines above 323 cm. This is associated with increased numbers of fragmented planktic foraminifera. There is a marked decline in foraminiferal abundance and the presence of partially dissolved benthic foraminifera at 281 cm. The lowest foraminiferal abundances and dissolved benthic foraminifera are observed between 281 and 161 cm, which is the interval with largest B-P ^{14}C age offsets.

To summarize, intervals of poor preservation and lower carbonate abundance occur in the latest glacial and early deglacial section of each core, and in VM21-30 extend through the deglacial section. The most pronounced decline in preservation occurs during the early deglacial section of all three cores.
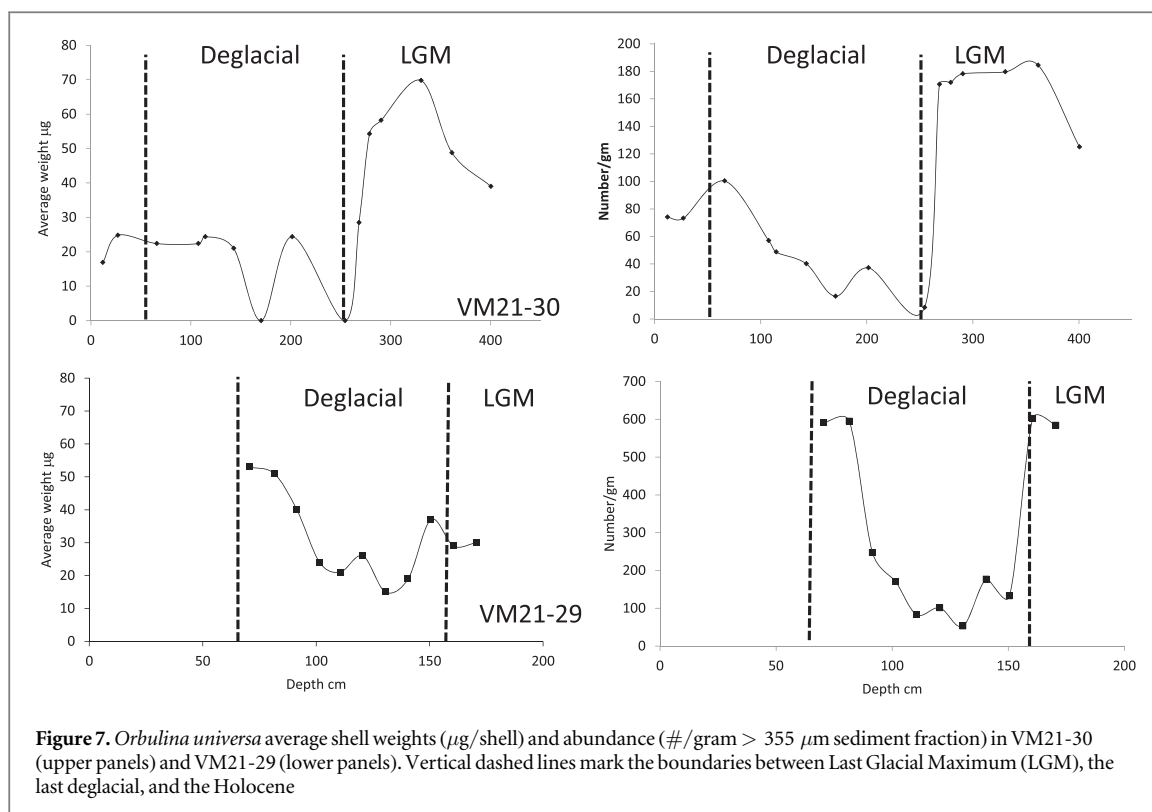
3.4. *Orbulina universa* shell weights and abundance as a proxy for carbonate ion variability

The abundance of *O. universa* drops dramatically across the glacial termination (figure 7). A similarly striking change in abundance is also observed in the VM21-29 core (figure 7). In the late glacial samples of VM21-29 the abundance of *O. universa* is ~600 specimens per gram and then drops to between 100 and 200

specimens per gram in the deglacial. In both VM21-30 and VM21-29, the abundance of *O. universa* returns to higher numbers in the late deglacial and Holocene sections.

The reduced abundance in *O. universa* in the latest glacial and deglacial samples is accompanied by a dramatic drop in the average shell weight of individual *O. universa* specimens (figure 7). In VM21-30 the weights drop by approximately 50% in the latest glacial and deglacial samples. The lowest shell weights are also observed in the deglacial samples of the VM21-29 core (figure 7). In the VM21-30 core, the late deglacial and Holocene shell weights do not return to the higher values seen in the glacial samples, whereas in the VM21-29 core the late deglacial weights increase to more than double the weight of the early to mid-deglacial specimens (figure 7).

In culture experiments (Bijma *et al* 1999, Bijma *et al* 2002) shell weights of the surface-dwelling *O. universa* drop by ~50% when $[CO_3{}^{2-}]$ is reduced by about 50%. The fact that the shell weights in our samples dropped by 50% from the late glacial to deglacial implies a comparably large drop in $[CO_3{}^{2-}]$ in surface waters of the EEP during the late glacial and deglaciation. In the EEP today surface ocean $[CO_3{}^{2-}]$ values are 225–275 mmol m^{-3} (Lovenduski *et al* 2015). Interannual variations in $[CO_3{}^{2}]$ accompanies changes in upwelling associated with ENSO, but those changes are small in comparison to the ~50% change implied by the *O. universa* shell weights. We also acknowledge that the magnitude of carbonate ion change within the water column implied by the abundance drop and the shell weight drop seen in the VM21-30 and VM21-29 records may be exaggerated due to dissolution on the seafloor, which would bias an explicit estimate of carbonate ion change.

Figure 7. *Orbulina universa* average shell weights (μg/shell) and abundance (#/gram > 355 μm sediment fraction) in VM21-30 (upper panels) and VM21-29 (lower panels). Vertical dashed lines mark the boundaries between Last Glacial Maximum (LGM), the last deglacial, and the Holocene
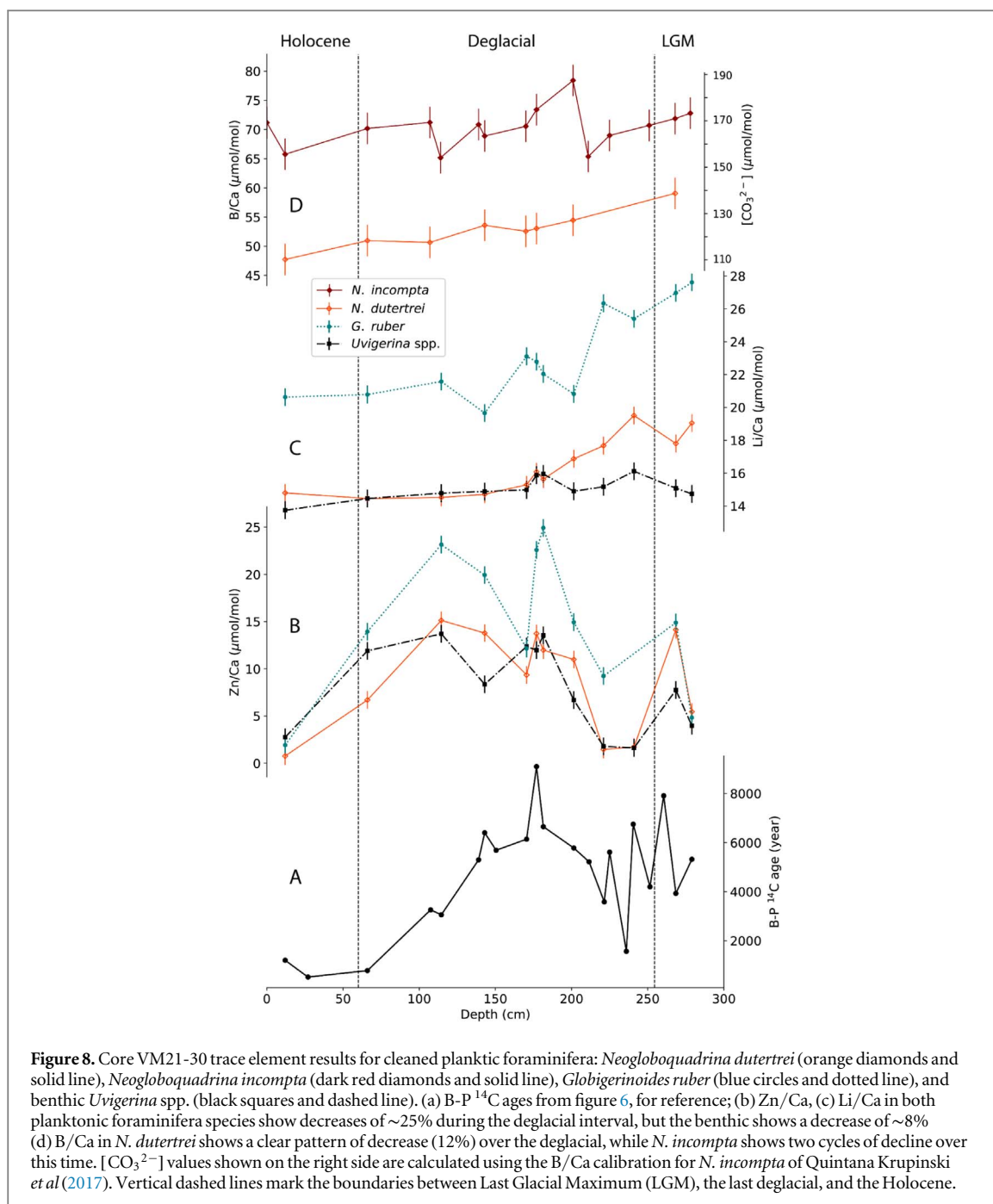
3.5. Trace element estimates of carbonate ion variability

In VM21-30, the B/Ca values of *N. dutertrei* decrease by ~12% across the entire deglacial section, while the thermocline-to-near-surface dwelling *N. incompta* B/Ca values show two shorter cycles of decline and rise during the deglacial, with minima at 211 and 114 cm (figure 8). It should be noted that while some planktic B/Ca can be altered by post-depositional dissolution, dissolution does not affect the B/Ca of *N. dutertrei* or *N. incompta* (Dai *et al* 2016, Quintana Krupinski *et al* 2017). A lack of correlation ($r^2 < 0.08$, <0.02, and <0.01, respectively) between B/Ca and elements used to monitor contamination (Fe/Ca, Mn/Ca, Al/Ca) implies the B/Ca trends do not reflect contamination; the same is true for Li/Ca ($r^2 < 0.12$, <0.22, and <0.32, respectively). Using the B/Ca-[CO_3^{2-}] calibration of Quintana Krupinski *et al* (2017) (B/Ca = [CO_3^{2-}] * 0.420–0.173), B/Ca values for the whole VM21-30 record translate to [CO_3^{2-}] values between ~155 μmol kg^{-1} (114 cm) and ~190 μmol kg^{-1} (201 cm) (figure 8); similarly low [CO_3^{2-}] values occur in the deglacial section of VM21-29 (table S5). However, modern [CO_3^{2-}] values at the calcification depth of *N. incompta* are ~170–180 μmol kg^{-1} (Quintana Krupinski *et al* 2017). The *N. incompta* data document two long intervals of anomalously low B/Ca in the deglacial section, indicative of [CO_3^{2-}] values well below modern values.

No calibration yet exists for *N. dutertrei*, but the range of B/Ca values in this record agree well with those reported for this species by Foster (2008).

Applying the Quintana Krupinski *et al* (2017) calibration to *N. dutertrei* indicates a steady [CO_3^{2-}] decline from high values of ~140 μmol kg^{-1} in the glacial period to low values of ~115 μmol kg^{-1} in the Holocene. These values are consistently lower than those for *N. incompta* but *N. dutertrei* is known to form a gametogenic crust deeper in the water column and is commonly thought have a deeper habitat than *N. incompta*. Therefore, the *N. dutertrei* results may reflect lower [CO_3^{2-}] conditions at deeper water depths. Here too we acknowledge that release of excess carbon to the water column was likely discontinuous (see discussion on dissolution estimates) and because of this, it is also likely that the B/Ca results could be biased due to the dissolution of or reduced abundance of specimens that lived at times of highest carbon flux. Hence, we may not record a precise estimate of carbonate ion decline at times of highest carbon release. This would account for the fact that the carbonate ion change implied by the *O. universa* data appears much larger than is implied by the B/Ca data.

The Li/Ca values of *G. ruber* and *N. dutertrei* decrease by about 25% across the entire deglacial section of the VM21-30 core (figure 8). We rule out a temperature effect in this ~25% decrease in Li/Ca because if this decline were caused by rising temperature, it would require a surface and thermocline warming of ~6 °C (Hall and Chan 2004), whereas alkenone and Mg/Ca records indicate sea surface temperatures (SSTs) warmed during the glacial termination by no more than ~1 °C–2 °C in the EEP (Koutavas *et al* 2002, Koutavas and Lynch-Stieglitz 2003, Koutavas and Sachs 2008) (figure S2). In addition, much of

Figure 8. Core VM21-30 trace element results for cleaned planktic foraminifera: *Neogloboquadrina dutertrei* (orange diamonds and solid line), *Neogloboquadrina incompta* (dark red diamonds and solid line), *Globigerinoides ruber* (blue circles and dotted line), and benthic *Uvigerina* spp. (black squares and dashed line). (a) B-P ^{14}C ages from figure 6, for reference; (b) Zn/Ca, (c) Li/Ca in both planktonic foraminifera species show decreases of ~25% during the deglacial interval, but the benthic shows a decrease of ~8% (d) B/Ca in *N. dutertrei* shows a clear pattern of decrease (12%) over the deglacial, while *N. incompta* shows two cycles of decline over this time. $[CO_3^{2-}]$ values shown on the right side are calculated using the B/Ca calibration for *N. incompta* of Quintana Krupinski *et al* (2017). Vertical dashed lines mark the boundaries between Last Glacial Maximum (LGM), the last deglacial, and the Holocene.

the drop in Li/Ca preceded the SST rise (figure S2; Koutavas and Sachs 2008). The Li/Ca changes therefore primarily reflect a decline in $[CO_3^{2-}]$ over the deglaciation.

3.6. Zn/Ca from VM21-30

The planktic and benthic records of Zn/Ca exhibit very different deglacial trends relative to Li/Ca or B/Ca. All species exhibit a broad maximum in Zn/Ca during the deglacial section of VM21-30 (figure 8). The Zn/Ca values among the foraminifera are also quite similar (figure 9), although the *G. ruber* Zn/Ca are ~5–10 μmol mol^{-1} higher throughout most of the record. The relatively high values of Zn/Ca in *G. ruber* during the deglacial section does not appear to reflect

contamination, or residual oxyhydroxide coatings on the foraminifera because other elemental data used for monitoring contamination remain low (for Al/Ca, Mn/Ca, and Fe/Ca, r^2 values are <0.29, <0.29, and <0.24, respectively, for all species).

Because the incorporation of Zn into foraminiferal calcite depends on both seawater [Zn] and on $[CO_3^{2-}]$, Zn/Ca is expected to vary with both variables. But both B/Ca and Li/Ca exhibit decreasing values over the deglacial section of the core and indicate declining $[CO_3^{2-}]$ whereas Zn/Ca values increase in the deglacial section, reaching a maximum in the mid-deglacial (figure 9). The consistent trends in the Zn/Ca from VM21-30 in both benthic and planktic species and the fact that it does not track the Li/Ca or
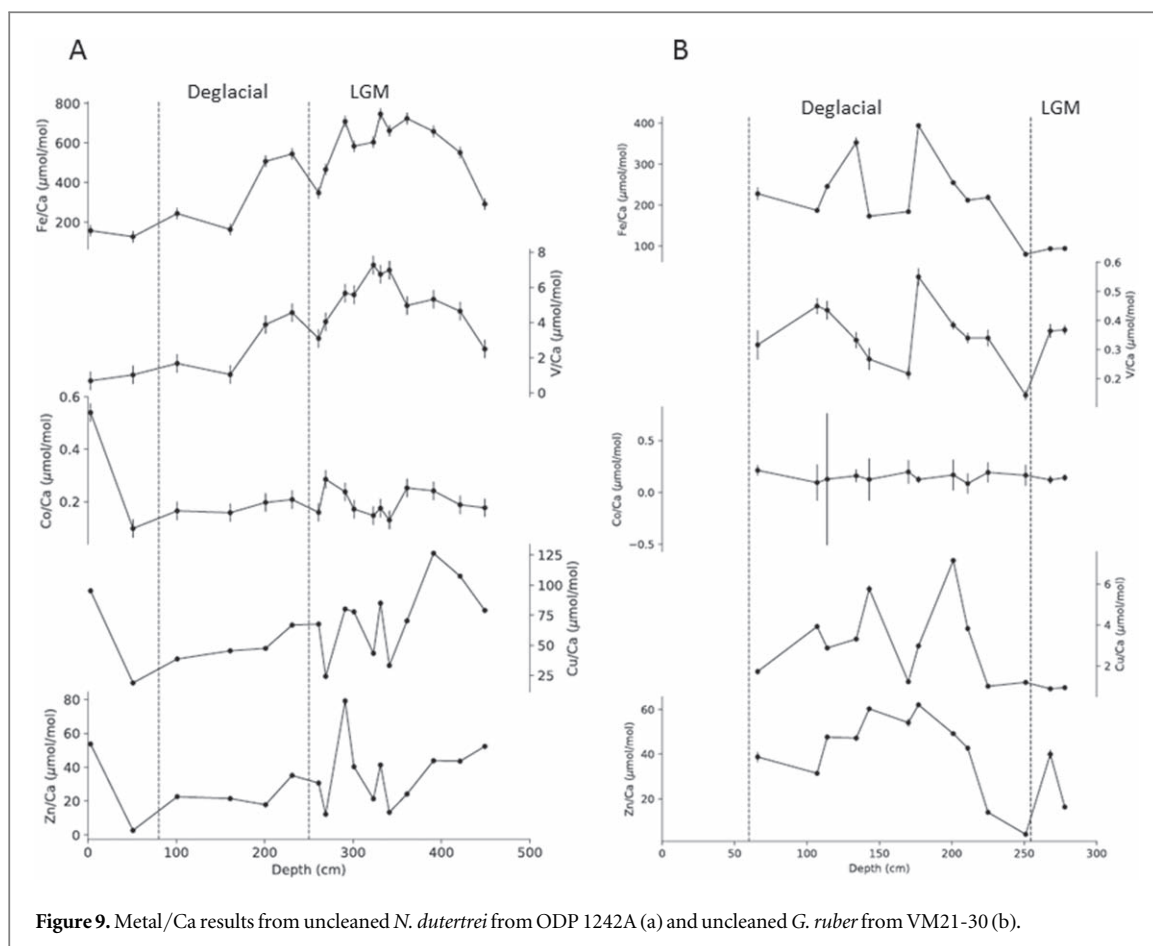
Figure 9. Metal/Ca results from uncleaned *N. dutertrei* from ODP 1242A (a) and uncleaned *G. ruber* from VM21-30 (b).
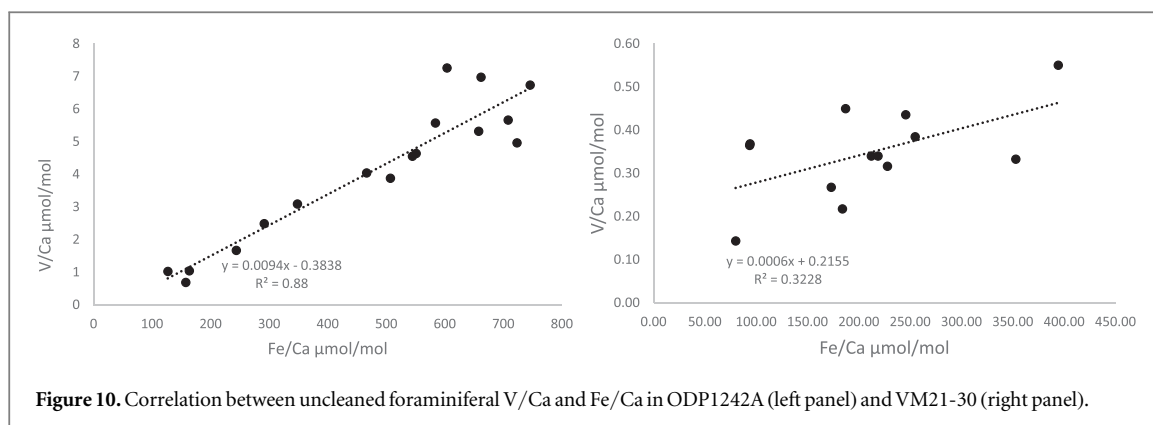
the B/Ca records leads us to conclude that the deglacial increase in Zn/Ca represents changes in seawater [Zn] rather than [CO_3^{2-}]. The increased Zn/Ca corresponds with the large decrease in Δ^{14}C implying that both share a common source.

3.7. Hydrothermal metal precipitates

Hydrothermal plume particles from vent fluids are highly enriched in metals. These particles are scavenged from and precipitated out of seawater near the vents. Therefore, variations in metal precipitates in sediments and foraminiferal coatings should reflect hydrothermal activity nearby. In contrast to measuring metal precipitate fluxes directly from sediments, measuring the elemental composition of foraminifera and their coatings has the advantage of circumventing complicating issues such as dilution by non-hydrothermal inputs and sediment focusing. And because we do not have independent measurements of a constant flux proxy such as ^{230}Th (Lund *et al* 2016, Costa *et al* 2017) we have instead normalized the elemental values to the foraminiferal calcium. In this way we document relative changes in abundance of hydrothermal metals rather than actual flux estimates. In these data we find that Fe/Ca and Zn/Ca values of the uncleaned foraminifera are ~5–20x higher than that of cleaned foraminifera from the same core (figure 9, table S6).

In the ODP1242A record (figure 9(A)), the highest El/Ca values occur in the glacial section; this is most pronounced for Fe/Ca and V/Ca. The higher Fe/Ca and V/Ca values also coincide with the largest B-P ages in this core. There is a strong correlation between Fe/Ca and V/Ca (figure 10), which agrees with modern studies that find scavenging of V by colloidal ferrihydrite in equal measure (Feely *et al* 1994, Cave *et al* 2002, German *et al* 2002, Dunk and Mills 2006). The Cu/Ca and Co/Ca values are more variable than Fe and V but the highest Cu/Ca values also occur late glacial section of ODP 1242A (figure 9(A)). The Zn/Ca values in ODP1242A glacial samples do not appear significantly higher in the late glacial section in association with the anomalous radiocarbon ages as is the case in the VM21-30 core. The only explanation we can suggest is that the Zn content of hydrothermal fluids near the ODP sites were different than those near the VM-21-30 sites.

In the VM21-30 core the highest El/Ca values are centered in the deglacial section (figure 9(B)), and deglacial maxima occur in both Zn/Ca (6X higher) and in Cu/Ca (3X higher) compared to values in the glacial section (figure 9(A)). These maxima in VM21-30 El/Ca also coincide with the largest B-P ages, as they do in the ODP1242A core. The Cu/Ca and Co/Ca values more variable with less pronounced enrichment in the LGM and early deglacial section of VM21-30. The Cu/Ca values in VM21-30 are one to

Figure 10. Correlation between uncleaned foraminiferal V/Ca and Fe/Ca in ODP1242A (left panel) and VM21-30 (right panel).

two orders of magnitude lower than at ODP1242A and Co/Ca values are largely invariant. Still, some coherence between Cu/Ca with Fe/Ca and V/Ca can be explained by the co-precipitation of these elements with iron oxyhydroxides (Dunk and Mills 2006). And it is clear from a comparison between the ODP1242A and VM21-30 results that the flux of these hydrothermally derived metals varied across the EEP, with higher amounts of metal accumulation in the late glacial near the ODP1242A site and later lower amounts during the deglacial near the VM21-30 site.

4. Discussion

In the late 1970s the plate tectonics theory gained strong support from oceanographic data collected by the Deep-Sea Drilling Program and other initiatives that acquired sea floor observations, including magnetic reversals and biostratigraphic data that documented increasing ages of the sediments overlying basaltic crust away from the mid-Atlantic mountain chain. The discovery of 'thermal springs' along the Galapagos Rift during the late 1970s (Corliss *et al* 1979) still stands as one of the most transformative discoveries of that era. That initial discovery at the Galapagos Rift did not quantify the actual flux of CO_2 emanating from the 'thermal springs'. But the measurements of alkalinity and pH indicated those springs carried a significant amount of CO_2 (Corliss *et al* 1979). It has taken many decades since that original discovery to obtain what is still a very sparse database of observations from the boundaries of active tectonic plates where much of the geologic activity and hydrothermalism occurs. That sparse observational database leaves considerable uncertainty about how vents contribute to the overall carbon budget of the oceans. It is in this long-term context of exploration that the discovery of liquid and solid CO_2 reservoirs stands-out as an important advance. These discoveries, together with geologic observations of variable hydrothermalism during the Pleistocene glacial cycles make it clear that processes that regulate the flux of carbon from the Earth's interior to its exterior are not spatially uniform nor are they necessarily slow and continuous. Thus, there

remains much to learn about what regulates the flux and accumulation of hydrothermal carbon. The question of whether the accumulation and variable flux of geologic carbon to the ocean from these sources influenced the global carbon cycle on glacial/interglacial time scales remains an incipient hypothesis to be tested. Towards that goal, we evaluated whether there was increased flux of hydrothermal carbon to the ocean during the last glacial termination. The findings presented here are compelling evidence that there was increased flux of hydrothermally-derived carbon to the ocean in the EEP at the last glacial termination. This has important implications for the history of atmospheric pCO_2 and $\Delta^{14}C$ because the EEP is a primary conduit for exchange of carbon between the ocean to the atmosphere.

The results do not put constraint on the amount of hydrothermal carbon released to the surface ocean in the EEP during the last glacial termination but the magnitudes of change in radiocarbon, $\delta^{13}C$ and trace elements implies a large amount of carbon was released over thousands of years that would have contributed to the higher ΔpCO_2 documented in boron isotope records (Martinez-Boti *et al* 2015). The dissolution of carbonates at 600 meters in the EEP alone is strong evidence that there was large flux of carbon into the upper ocean that altered the carbonate chemistry. The *O. universa* shell weight data also imply a drop of surface ocean $[CO_3^{2}]$ that may have been as much as 50%. The planktic foraminiferal B/Ca and Li/Ca data presented here also indicate a large increased flux of carbon into the surface ocean that lowered the carbonate saturation. Together with boron isotope results, our findings indicate geologic carbon would have been a significant fraction of the carbon released from the ocean to the atmosphere at the last glacial termination.

In the modern ocean the VM21-29 and VM21-30 sites are above the calcite lysocline and close to the aragonite lysocline in the EEP. The variable dissolution evident in benthic foraminifera implies that the carbonate saturation in the EEP intermediate waters dropped sometimes during the late glacial and deglaciation. This implies episodic upwelling of ^{14}C-depleted,

CO_2-rich waters in the EEP during the late glacial and early deglacial. This is consistent with large range of ^{14}C ages and very old reservoir ages among planktic foraminifera within the late glacial and deglacial samples.

The large B-P ^{14}C age anomalies and increased surface ocean reservoir ages together with the increased accumulation of hydrothermal metals is evidence that the source of excess carbon that affected the carbonate changes was from a hydrothermal source and not from respired metabolic carbon. The large enrichment of Zn in both the foraminiferal calcite and in oxide coatings, along with the enrichment and co-variation of Fe and V indicates there was a hydrothermal source nearby. The oxide coatings would have formed after deposition at the sea floor. However, the elevated Zn/Ca in the cleaned planktic and benthic foraminifera of VM21-30 in the deglacial section indicates there was a large enrichment of dissolved Zn throughout the water column. The most likely source of this Zn would be from hydrothermal systems. However, it is not possible to infer from what hydrothermal system the Zn came. The fact that Zn is elevated throughout the water column over the deglacial implies there was a persistent supply. And this input of Zn coincided with the input of 'old' carbon. At the present time there is no known occurrence of liquid CO_2 at the hydrothermal vents in the EEP or on the margins of the Galapagos that might act as a supply of these metals during the deglacial. But it is worth noting that supercritical CO_2 (SFC-CO_2) is a highly efficient solvent for extraction of heavy metals (Lin *et al* 2014). Therefore, if there was SCF-CO_2 formed at depth beneath the hydrothermal or volcanic systems in the EEP, it could act as an efficient source for Zn and other metals. This is obviously a question that will require additional research. But the elevated Zn/Ca and 'very old' carbon recorded by carbonates in the EEP points to a geologic source of carbon.

The results presented here point to a large amount of hydrothermal carbon released at times during the last glacial termination and that carbon upwelled to the surface, but the changes in carbonate chemistry were likely also responding to changes in the upwelling intensity (Koutavas *et al* 2002, Koutavas and Lynch-Stieglitz 2003, Koutavas and Sachs 2008) that indicates stronger upwelling. The stronger upwelling documented in previous studies and the geochemical anomalies documented here coincided with elevated ΔpCO_2 in the EEP (Martinez-Boti *et al* 2015). It therefore appears that there were two factors affecting the flux of carbon to the surface ocean and atmosphere from the EEP during the glacial termination: episodic release of geologic carbon to the intermediate waters, and intensified upwelling. Because the EEP is one of the primary conduits for exchange of carbon from the ocean to the atmosphere our findings require reconsideration of the prevailing view about where the ocean released excess carbon to the atmosphere at the glacial

termination. The results also underscore the need to investigate other sites for evidence of geologic carbon release.

The present study does not put a constraint on the mechanism responsible for the increased flux of hydrothermal carbon at the glacial termination. The two prevailing ideas, sea level forcing (Lund and Asimow 2011, Huybers and Langmuir 2017) and temperature induced changes in hydrothermal carbon storage (Stott and Timmermann 2011) require additional evaluation. In that effort it will be important to conduct benthic carbon flux measurements on the flanks of active hydrothermal systems to quantify how these carbon sources contribute to the ocean's carbon budget. It will also be important to investigate trace metal concentrations at sites where there is known sources of SFC-CO_2 such as in the western tropical Pacific (Lupton *et al* 2008). Earth System Models may also offer opportunities to evaluate how point sources of carbon to the atmosphere such as the upwelling system in the EEP influence the global carbon cycle, including the carbonate system. Such experiments could then be compared with the growing database of observations that include proxies for carbonate ion and pH.

5. Conclusions

In this study we present evidence of increased carbon flux to the upper ocean within the upwelling region of the EEP at the glacial termination. The geochemical measurements support the suggestion that hydrothermal carbon contributed significantly to that increased carbon flux. When combined with results of previous research, it also appears that the increased flux of geologic carbon to the EEP was accompanied by enhanced upwelling strength in one of the ocean's primary conduits for exchange of carbon with the atmosphere. We conclude that the prevailing view that glacial/interglacial pCO_2 variability that characterized the glacial/interglacial cycles was controlled by the storage and subsequent ventilation of respired marine metabolic carbon must be modified to include geological processes that affect the flux of carbon from hydrothermal sources. We further conclude that there is vital importance in learning what regulates the flux of hydrothermal carbon to the ocean. This will require research that explores where and how geologic carbon is stored in the ocean basins and measurements of the actual fluxes of carbon from these sources that can better constrain the marine carbon budget. This research will not only advance knowledge about one of the major scientific challenges in Climate Science but will also provide important constraints on how the marine carbon cycle may be affected by warmer global temperatures in Earth's future.

Acknowledgments

ORCID iDs

Lowell D Stott ⓘ https://orcid.org/0000-0002-2025-0731

References

Al-Ammar A S, Gupta R K and Barnes R M 2000 Elimination of boron memory effect in inductively coupled plasma-mass spectrometry by ammonia gas injection into the spray chamber during analysis *Spectrochim. Acta* B **55** 629–35

Allen K A, Hönisch B, Eggins S M and Rosenthal Y 2012 Environmental controls on B/Ca in calcite tests of the tropical planktic foraminifer species globigerinoides ruber and globigerinoides sacculifer *Earth Planet. Sci. Lett.* **351–352** 270–80

Archer D, Winguth A, Lea D and Mahowald N 2000 What caused the glacial/interglacial atmospheric pCO_2 cycles? *Rev. Geophys.* **38** 159–89

Barker S, Greaves M and Elderfield H 2003 A study of cleaning procedures used for foraminiferal Mg/Ca paleothermometry *Geochem. Geophys. Geosyst.* **4** 8407

Beaulieu S E, Baker E T and German C R 2015 Where are the undiscovered hydrothermal vents on oceanic spreading ridges? *Deep Sea Res.* II **121** 202–12

Benway H M, Mix A C, Haley B A and Klinkhammer G P 2006 Eastern Pacific warm pool paleosalinity and climate variability: 0–30 ky *Paleoceanography* **21** PA3008

Berger W H 1982 Increase of carbon dioxide in the atmosphere during deglaciation: the coral reef hypothesis *Naturwissenschaften* **69** 87–8

Bijma J, Hönisch B and Zeebe R E 2002 Impact of the ocean carbonate chemistry on living foraminiferal shell weight: comment on 'Carbonate ion concentration in glacial-age deep waters of the Caribbean Sea' by W. S. Broecker and E. Clark *Geochem. Geophys. Geosyst.* **3** 1–7

Bijma J, Spero H J and Lea D W 1999 Reassessing foraminiferal stable isotope geochemistry: impact of the oceanic carbonate system (experimental results) *Use of Proxies in Paleoceanography: Examples from the South Atlantic* ed G Fischer and G Wefer (Berlin: Springer) pp 489–512

Bostock H C, Opdyke B N, Gagan M K and Fifield L K 2004 Carbon isotope evidence for changes in Antarctic intermediate water circulation and ocean ventilation in the southwest Pacific during the last deglaciation *Paleoceanography* **19** PA4013

Boyle E A 1981 Cadmium, zinc, copper, and barium in foraminifera tests *Earth Planet. Sci. Lett.* **53** 11–35

Boyle E A 1983 Manganese carbonate overgrowths on foraminifera tests *Geochim. Cosmochim. Acta* **47** 1815–9

Broecker W S, Yu J and Putnam A E 2015 Two contributors to the glacial CO_2 decline *Earth Planet. Sci. Lett.* **429** 191–6

Bryan S P and Marchitto T M 2008 Mg/Ca-temperature proxy in benthic foraminifera: new calibrations from the Florida Straits and a hypothesis regarding Mg/Li *Paleoceanography* **23** PA2220

Bryan S P, Marchitto T M and Lehman S J 2010 The release of ^{14}C-depleted carbon from the deep ocean during the last deglaciation: evidence from the Arabian Sea *Earth Planet. Sci. Lett.* **298** 244–54

Burton M R, Sawyer G M and Granieri D 2013 Deep carbon emissions from volcanoes *Rev. Mineralogy Geochem.* **75** 323–54

Camilli R, Nomikou P, Escartín J, Ridao P, Mallios A, Kilias S P and Argyraki A 2015 The Kallisti Limnes, carbon dioxide-accumulating subsea pools *Sci. Rep.* **5** 12152

Cave R R, German C R, Thomson J and Nesbitt R W 2002 Fluxes to sediments underlying the Rainbow hydrothermal plume at 36°14′N on the mid-atlantic ridge *Geochim. Cosmochim. Acta* **66** 1905–23

Christopher V, Claude H, Esteban G, Dennis G and Karen H 2013 Lithological structure of the Galápagos plume *Geochem. Geophys. Geosyst.* **14** 4214–40

Corliss J B *et al* 1979 Submarine thermal springs on the Galápagos rift *Science* **203** 1073–83

Costa K M, McManus J F, Middleton J L, Langmuir C H, Huybers P J, Winckler G and Mukhopadhyay S 2017 Hydrothermal deposition on the juan de fuca ridge over multiple glacial–interglacial cycles *Earth Planet. Sci. Lett.* **479** (Suppl. C) 120–32

Dai Y, Yu J and Johnstone H J H 2016 Distinct responses of planktic foraminiferal B/Ca to dissolution on seafloor *Geochem. Geophys. Geosyst.* **17** 1339–48

de la Fuente M, Skinner L, Calvo E, Pelejero C and Cacho I 2015 Increased reservoir ages and poorly ventilated deep waters inferred in the glacial eastern equatorial pacific *Nat. Commun.* **6** 7420

De Pol-Holz R, Keigwin L, Southon J, Hebbeln D and Mohtadi M 2010 No signature of abyssal carbon in intermediate waters off Chile during deglaciation *Nat. Geosci.* **3** 192–5

Doss W, Marchitto T M, Eagle R, Rashid H and Tripati A 2018 Deconvolving the saturation state and temperature controls on benthic foraminiferal Li/Ca, based on downcore paired B/Ca measurements and coretop compilation *Geochim. Cosmochim. Acta* **236** 297–314

Dunk R M and Mills R A 2006 The impact of oxic alteration on plume-derived transition metals in ridge flank sediments from the East Pacific Rise *Mar. Geol.* **229** 133–57

Feely R A, Gendron J F, Baker E T and Lebon G T 1994 Hydrothermal plumes along the East Pacific Rise, 8°40′ to 11° 50′N: particle distribution and composition *Earth Planet. Sci. Lett.* **128** 19–36

Fischer H *et al* 2010 The role of Southern ocean processes in orbital and millennial CO_2 variations—a synthesis *Q. Sci. Rev.* **29** 193–205

Foster G L 2008 Seawater pH, pCO_2 and $[CO_3^{2-}]$ variations in the Caribbean Sea over the last 130 kyr: a boron isotope and B/Ca study of planktic foraminifera *Earth Planet. Sci. Lett.* **271** 254–66

German C R, Colley S, Palmer M R, Khripounoff A and Klinkhammer G P 2002 Hydrothermal plume-particle fluxes at 13 °N on the East Pacific Rise *Deep Sea Res.* I **49** 1921–40

Hall J M and Chan L 2004 Ba/Ca in Neogloboquadrina pachyderma as an indicator of deglacial meltwater discharge into the western Arctic Ocean *Paleoceanography* **19** PA1017

Harpp K S and White W M 2018 Tracing a mantle plume: isotopic and trace element variations of Galápagos seamounts *Geochem. Geophys. Geosyst.* **2** 2000GC000137

Hathorne E C and James R H 2006 Temporal record of lithium in seawater: a tracer for silicate weathering? *Earth Planet. Sci. Lett.* **246** 393–406

Haynes L L, Hönisch B, Dyez K A, Holland K, Rosenthal Y, Fish C R, Subhas A V and Rae J W B 2017 Calibration of the B/Ca proxy in the planktic foraminifer Orbulina universa to Paleocene seawater conditions *Paleoceanography* **32** 580–99

Hendry K R, Rickaby R E M, Meredith M P and Elderfield H 2009 Controls on stable isotope and trace metal uptake in Neogloboquadrina pachyderma (sinistral) from an Antarctic sea-ice environment *Earth Planet. Sci. Lett.* **278** 67–77

Henehan M, Foster G L, Rae J W B, Prentice K C, Erez J, Bostock H C, Marshall B J and Wilson P A 2015 Evaluating the utility of B/Ca ratios in planktic foraminifera as a proxy for the carbonate system: A case study of Globigerinoides ruber *Geochem. Geophys. Geosyst.* **16** 1052–69

Holland K, Eggins S M, Hönisch B, Haynes L L and Branson O 2017 Calcification rate and shell chemistry response of the planktic foraminifer Orbulina universa to changes in microenvironment seawater carbonate chemistry *Earth Planet. Sci. Lett.* **464** 124–34

Howes E *et al* 2017 Decoupled carbonate chemistry controls on the incorporation of boron into Orbulina universa *Biogeosciences* **14** 415–30

Huybers P and Langmuir C H 2017 Delayed CO_2 emissions from mid-ocean ridge volcanism as a possible cause of late-Pleistocene glacial cycles *Earth Planet. Sci. Lett.* **457** 238–49

Inagaki F *et al* 2006 Microbial community in a sediment-hosted CO_2 lake of the southern Okinawa trough hydrothermal system *Proc. Natl Acad. Sci.* **103** 14164–9

Koutavas A and Lynch-Stieglitz J 2003 Glacial-interglacial dynamics of the eastern equatorial Pacific cold tongue-intertropical convergence zone system reconstructed from oxygen isotope records *Paleoceanography* **18** 1089

Koutavas A, Lynch-Stieglitz J, Marchitto T M and Sachs J P 2002 El Nino-like pattern in ice age tropical Pacific sea surface temperature *Science* **297** 226–30

Koutavas A and Sachs J P 2008 Northern timing of deglaciation in the eastern equatorial Pacific from alkenone paleothermometry *Paleoceanography* **23** PA4205

Lear C H and Rosenthal Y 2006 Benthic foraminiferal Li/Ca: Insights into Cenozoic seawater carbonate saturation state *Geol. Soc. Am.* **34** 985–8

Lear C H, Mawbey E M and Rosenthal Y 2010 Cenozoic benthic foraminiferal Mg/Ca and Li/Ca records: toward unlocking temperatures and saturation states *Paleoceanography* **25** PA4215

Levin L A *et al* 2016 Hydrothermal vents and methane seeps: rethinking the sphere of influence *Front. Mar. Sci.* **3** 72

Lin F, Liu D, Maiti Das S, Prempeh N, Hua Y and Lu J 2014 Recent progress in heavy metal extraction by supercritical CO_2 fluids *Ind. Eng. Chem. Res.* **53** 1866–77

Lovenduski N S, Long M and Lindsay K 2015 Natural variability in the surface ocean carbonate ion concentration *Biogeosciences* **12** 6321–35

Lund D C and Asimow P D 2011 Does sea level influence mid-ocean ridge magmatism on Milankovitch timescales? *Geochem. Geophys. Geosyst.* **12** Q12009

Lund D C, Asimow P D, Farley K A, Rooney T O, Seeley E, Jackson E W and Durham Z M 2016 Enhanced East Pacific Rise hydrothermal activity during the last two glacial terminations *Science* **351** 478–82

Lupton J *et al* 2006 Submarine venting of liquid carbon dioxide on a Mariana Arc volcano *Geochem. Geophys. Geosyst.* **7** Q08007

Lupton J, Lilley M, Butterfield D, Evans L, Embley R, Massoth G, Christenson B, Nakamura K and Schmidt M 2008 Venting of a separate CO_2-rich gas phase from submarine arc volcanoes: examples from the Mariana and Tonga-Kermadec arcs *J. Geophys. Res.* **113** B08S12

Marchitto T M, Curry W B and Oppo D W 2000 Zinc concentrations in benthic foraminifera reflect seawater chemistry *Paleoceanography* **15** 299–306

Marchitto T M, Oppo D W and Curry W B 2002 Paired benthic foraminiferal Cd/Ca and Zn/Ca evidence for a greatly increased presence of Southern ocean water in the glacial North Atlantic *Paleoceanography* **17** 1038

Marchitto T M, Lehman S J, Ortiz J D, Fluckiger J and van Geen A 2007 Marine radiocarbon evidence for the mechanism of deglacial atmospheric CO_2 rise *Science* **316** 1456–9

Marriott C S, Henderson G M, Crompton R, Staubwasser M and Shaw S 2004 Effect of mineralogy, salinity, and temperature on Li/Ca and Li isotope composition of calcium carbonate *Chem. Geol.* **212** 5–15

Martin P A and Lea D W 2002 A simple evaluation of cleaning procedures on fossil benthic foraminiferal Mg/Ca *Geochem. Geophys. Geosyst.* **3** 8401

Martinez-Boti M A, Marino G, Foster G L, Ziveri P, Henehan M J, Rae J W B, Mortyn P G and Vance D 2015 Boron isotope evidence for oceanic carbon dioxide leakage during the last deglaciation *Nature* **518** 219–22

Muscheler R, Beer J, Wagner G, Laj C, Kissel C, Raisbeck G M, Yiou F and Kubik P W 2004 Changes in the carbon cycle during the last deglaciation as indicated by the comparison of ^{10}Be and ^{14}C records *Earth Planet. Sci. Lett.* **219** 325–40

Nealson K 2006 Lakes of liquid CO_2 in the deep sea *Proc. Natl Acad. Sci.* **103** 13903–4

Petrenko V V *et al* 2016 Measurements of 14C in ancient ice from Taylor Glacier, Antarctica constrain *in situ* cosmogenic ^{14}CH₄ and ^{14}CO production rates *Geochim. Cosmochim. Acta* **177** 62–77

Quintana Krupinski N B, Russell A D, Pak D K and Paytan A 2017 Core-top calibration of B/Ca in Pacific ocean neogloboquadrina incompta and globigerina bulloides as a surface water carbonate system proxy *Earth Planet. Sci. Lett.* **466** 139–51

Reimer P J *et al* 2013 IntCal13 and marine13 radiocarbon age calibration curves 0–50 000 years cal BP *Radiocarbon* **55** 1869–87

Ronge T A, Tiedemann R, Lamy F, Kohler P, Alloway B V, De Pol-Holz R, Pahnke K, Southon J and Wacker L 2016 Radiocarbon constraints on the extent and evolution of the South Pacific glacial carbon pool *Nat. Commun.* **7** 11487

Rosenthal Y, Field M P and Sherrell R M 1999 Precise determination of element/calcium ratios in calcareous samples using sector field inductively coupled plasma mass spectrometry *Anal. Chem.* **71** 3248–53

Sakai H, Gamo T, Kim E-S, Tsutsumi M, Tanaka T, Ishibashi J, Wakita H, Yamano M and Oomori T 1990 Venting of carbon dioxide-rich fluid and hydrate formation in mid-okinawa trough backarc basin *Science* **248** 1093–6

Salazar J M L, Hernández P A, Pérez N M, Melián G, Álvarez J, Segura F and Notsu K 2001 Diffuse emission of carbon dioxide from Cerro Negro Volcano, Nicaragua, Central America *Geophys. Res. Lett.* **28** 4275–8

Schmitt J *et al* 2012 Carbon isotope constraints on the deglacial CO_2 rise from ice cores *Science* **336** 711–4

Sigman D M and Boyle E A 2000 Glacial/interglacial variations in atmospheric carbon dioxide *Nature* **407** 859–69

Spero H J and Lea D W 2002 The cause of carbon isotope minimum events on glacial terminations *Geochim. Cosmochim. Acta* **66** A731–731

Stern J V and Lisiecki L E 2014 Termination 1 timing in radiocarbon-dated regional benthic δ^{18}O stacks *Paleoceanography* **29** 1127–42

Stott L, Cannariato K, Thunell R, Haug G H, Koutavas A and Lund S 2004 Decline of surface temperature and salinity in the western tropical Pacific Ocean in the Holocene epoch *Nature* **431** 56–9

Stott L, Southon J, Timmermann A and Koutavas A 2009 Radiocarbon age anomaly at intermediate water depth in the Pacific Ocean during the last deglaciation *Paleoceanography* **24** PA2223

Stott L and Timmermann A 2011 Hypothesized link between glacial/interglacial atmospheric CO_2 cycles and storage/release CO_2-rich fluids from the deep sea *Geophysical Monograph Series: Understanding the Causes, Mechanisms and Extent of the Abrupt Climate Change* (Washington, DC: American Geophysical Union) (https://doi.org/10.1029/2010GM001052)

Takahashi T *et al* 2009 Climatological mean and decadal change in surface ocean pCO₂, and net sea–air CO_2 flux over the global oceans *Deep Sea Res.* II **56** 554–77

Tolstoy M 2015 Mid-ocean ridge eruptions as a climate valve *Geophys. Res. Lett.* **42** 1346–51

Umling N E and Thunell R C 2017 Synchronous deglacial thermocline and deep-water ventilation in the eastern equatorial Pacific *Nat. Commun.* **8** 14203

van Dijk I, de Nooijea L J, Wolthers M and Reichart G-J 2017 Impacts of pH and $[CO_3^{2-}]$ on the incorporation of Zn in foraminiferal calcite *Geochim. Cosmochim. Acta* **197** 263–77

Wara M W, Delaney M L, Bullen T D and Ravelo A C 2003 Possible roles of pH, temperature, and partial dissolution in determining boron concentration and isotopic composition in planktic foraminifera *Paleoceanography* **18** 1100

Yu J, Elderfield H and Hönisch B 2007 B/Ca in planktic foraminifera as a proxy for surface seawater pH *Paleoceanography* **22** PA2202

Yu J, Thornalley D J R, Rae J W B and McCave N I 2013 Calibration and application of B/Ca, Cd/Ca, and δ^{11}B in Neogloboquadrina pachyderma (sinistral) to constrain CO_2 uptake in the subpolar North Atlanti *Paleoceanography* **28** 237–52